Analogue cosmological particle creation: Quantum correlations in expanding Bose-Einstein condensates

Angus Prain,[1,*] Serena Fagnocchi,[2,†] and Stefano Liberati[1,‡]

[1]*SISSA, Via Bonomea 265, 34136 Trieste, Italy, and INFN sezione di Trieste, Via Valerio 2, 34127 Trieste, Italy*
[2]*School of Physics & Astronomy, University of Nottingham, University Park, Nottingham NG7 2RD, United Kingdom*

We investigate the structure of quantum correlations in an expanding Bose-Einstein condensate (BEC) through the analogue gravity framework. We consider both a $3 + 1$ isotropically expanding BEC as well as the experimentally relevant case of an elongated, effectively $1 + 1$ dimensional, expanding condensate. In this case we include the effects of inhomogeneities in the condensate, a feature rarely included in the analogue gravity literature. In both cases we link the BEC expansion to a simple model for an expanding spacetime and then study the correlation structure numerically and analytically (in suitable approximations). We also discuss the expected strength of such correlation patterns and experimentally feasible BEC systems in which these effects might be detected in the near future.

I. INTRODUCTION

Within the framework of quantum field theory in curved spacetime where fields propagate on a fixed background, some interesting—and sometimes surprising—quantum instabilities are predicted. Among them a crucial role has been played by the so-called *cosmological particle creation*: a quantum emission of particles as a consequence of an expansion of spacetime [1,2]. Being associated with wave propagation over a dynamical space and not (when backreaction is neglected) to a property of the Einstein equations, it is not peculiar to the gravitational framework but appears as a quantum field nonequilibrium process in a diverse range of physical systems. This is a feature shared with other semiclassical emissions, for example, Hawking radiation [3]. For this reason, recently there has been growing interest in studying such nontrivial quantum effects in a laboratory setting with condensed matter systems, a field of research that goes under the general name of ''analogue models of gravity'' (see e.g. [4] for an extensive review).

In particular, the propagation of linearized acoustic perturbations on an inviscid and irrotational fluid can be shown to be described by the same equation of motion as that which describes the propagation of a scalar field on a curved spacetime. Of course such ideal systems are not readily available in nature but it is possible to produce systems which, to a very good degree of approximation, do actually behave as perfect fluids. In recent years, a special role in this sense has been played by Bose-Einstein condensates (BEC), the basic observation being in this case that phase perturbations of the wave function describing a weakly interacting BEC are, in a certain limit, described by

a massless quantum scalar field propagating on a nontrivially curved background Lorenzian spacetime [4–6].

A BEC can therefore be used to simulate special gravitational backgrounds and the associated particle production such as Hawking radiation of black holes [7–10], or the cosmological emission mentioned above that we are concerned with in this paper. For example, releasing the trapping potential of a BEC appropriately [11–17] or modulating external parameters of the experimental setting [18–23], it is possible to induce the necessary dynamics which give rise to interesting background geometries. Because of the nontrivial time evolution, the system undergoes a nonequilibrium phase to which are associated quantum emissions whose spectrum strictly depends on the parameters modulating the evolution. This opens up the possibility of experimentally accessing new kinds of phenomena directly involving the quantum nature of cold atom systems as well as providing additional insights on the general mechanisms of such emissions in the gravitational case.

Cast in a different light, this possibility of describing terrestrial experiments using a curved spacetime analogue provides one with a new set of tools to tackle difficult problems in condensed matter physics and is able to suggest new and interesting nonequilibrium quantum effects. Moreover, a successful application of these alternative techniques and consequent observation of the effects predicted would serve as further theoretical support for the validity of the semiclassical theory. The issue of how to practically observe these quantum emissions and verify their origin is a crucial point in the condensed matter literature. In particular, there has been recently a large interest in the calculation and measurement of correlation patterns in expanding condensates to access these quantum effects (for example, see [24–26]). In [8] it has been proposed that evidence for analogue Hawking emission in a sonic black hole manifested in a BEC might be

---
[*]aprain@sissa.it
[†]fagnocchi@nottingham.ac.uk
[‡]liberati@sissa.it

solicited by measuring the two point correlation structure associated with the quantized density or phase perturbation fields. The idea is that the correlation pattern should display a peculiar signature of the type of emission expected from black holes. Following the same line of reasoning, we apply this idea to analogue cosmological emission and attempt to isolate a cosmological signal in the correlation pattern in an expanding BEC.

In particular, this article is concerned with the experimentally accessible correlations between the phase and density perturbations in a BEC which are born during the expansion of the underlying gas both in the widely studied effectively $1 + 1$ dimensional "cigar"-shaped geometry and in a homogeneous expanding BEC. Such BEC systems are of theoretical interest in their own right and correlation measurements are experimentally accessible with the current technology [24–26]. Therefore it is possible that these systems will provide in the near future an arena within which to experimentally address interesting and new nonequilibrium quantum effects while at the same time shed light on the physics of quantum fields in expanding spacetime without using telescopes.

In the first section we collect and contextualize some results relevant for the study of correlations in an expanding BEC, reviewing how the analogy is applied to BEC and the dynamics of an expanding BEC. In the second section we compute the correlation structure for a massless scalar field in a particular expanding background spacetime in $3 + 1$D and show how to interpret such a result in terms of both an isotropically expanding $3 + 1$D condensate and a BEC with a time-dependent scattering length. We shall develop a general formalism for probing the effect of particle production (Bogoliubov coefficients) on correlations as embodied in the equal-time Wightman functions. In this context we shall derive results which are completely generic to particle production in any spatially translation invariant system, which can be applied to standard cosmologies as much as to "analogue spacetimes." In the third and final section which represents the main result of this article using both analytic and numerical methods, we discuss the structure of correlations in an anisotropically expanding, effectively $1 + 1$-dimensional, BEC. In particular, we shall derive the general, finite size, $1 + 1$-dimensional, equal-time Wightman function relevant for the cigar-shaped expanding BEC presently realized in experiments. We conclude with some proposals for improving the observability in practice of the correlation signal.

II. BACKGROUND

A. A BEC as an analogue spacetime

In this article we consider a weakly interacting BEC trapped in an attractive harmonic potential. Given the by now standard usage of this system as an analogue model of gravity, we limit ourselves to a summary of the salient

equations which we shall need in what follows, directing the reader to the extant literature for further reading [4–6].

In the dilute gas approximation, one can describe a Bose gas through a quantum field $\hat{\Psi}$ satisfying

$$i\hbar \frac{\partial}{\partial t} \hat{\Psi} = \left(-\frac{\hbar^2}{2m} \nabla^2 + V_{\text{ext}}(\mathbf{x}) + g(\bar{a})\hat{\Psi}^\dagger \hat{\Psi} \right)\hat{\Psi}. \quad (2.1)$$

Here m is the mass of the constituents, g parametrizes the strength of the interactions between pairs of bosons in the gas, and $\bar{a}$ is the scattering length of the atoms in an s-wave approximation. The former can be reexpressed in terms of the scattering length as

$$g(\bar{a}) = \frac{4\pi\bar{a}\hbar^2}{m}. \quad (2.2)$$

Adopting a mean field approximation, the quantum field can be separated into a macroscopic (classical) condensate (called the wave function of the condensate) and a fluctuation: $\hat{\Psi} = \psi + \hat{\varphi}$, with $\langle \hat{\Psi} \rangle = \psi$. Then, by adopting the self-consistent mean field approximation and neglecting backreaction effects of the quantum fluctuations on the condensate, one obtains the Gross-Pitaevskii (GP) equation of motion for the wave function of the condensate,

$$i\hbar \frac{\partial \psi}{\partial t} = -\frac{\hbar^2}{2m} \nabla^2 \psi + V_{\text{ext}} \psi + g(\bar{a})|\psi|^2 \psi. \quad (2.3)$$

Now, adopting the Madelung representation for the wave function of the condensate [27]

$$\psi(t, \mathbf{x}) = \sqrt{\rho(t, x)} \exp[-i\theta(t, x)/\hbar], \quad (2.4)$$

where $\rho = \psi^* \psi$ is the condensate density, and defining an irrotational "velocity field" by $\mathbf{v} := \nabla\theta/m$, the Gross-Pitaevskii equation can be rewritten as a continuity equation plus an Euler equation:

$$\frac{\partial}{\partial t}\rho + \nabla \cdot (\rho\mathbf{v}) = 0, \quad (2.5)$$

$$m\frac{\partial}{\partial t}\mathbf{v} + \nabla\left(\frac{mv^2}{2} + V_{\text{ext}}(t, \mathbf{x}) + g\rho - \frac{\hbar^2}{2m} \frac{\nabla^2\sqrt{\rho}}{\sqrt{\rho}} \right) = 0. \quad (2.6)$$

These equations are completely equivalent to those of an irrotational and inviscid fluid apart from the presence of the so-called quantum potential,

$$V_{\text{quantum}} = -\hbar^2 \nabla^2\sqrt{\rho}/(2m\sqrt{\rho}), \quad (2.7)$$

which has the dimensions of an energy. It is then clear that, when small gradients of the background density are involved, this term can be safely neglected and a hydrodynamical approximation [also known as the Thomas Fermi (TF) approximation] holds.

We are concerned with the quantum excitations on top of the BEC background solution of the GP equation (or hydrodynamic equivalents). Inserting the mean field ansatz

in Eq. (2.1) and again neglecting backreaction, one obtains the equation for the operator valued perturbation:

$$i\hbar \frac{\partial}{\partial t} \hat{\varphi}(t, \mathbf{x}) = \left(-\frac{\hbar^2}{2m}\nabla^2 + V_{\text{ext}}(\mathbf{x}) + 2g\rho\right)\hat{\varphi}(t, \mathbf{x})$$
$$+ g\rho\hat{\varphi}^\dagger(t, \mathbf{x}). \tag{2.8}$$

The elementary excitations of this dynamical system are described by variables obtained by a Bogoliubov transformation from the fundamental field. This can be also shortcut by adopting the so-called quantum acoustic representation [4]

$$\hat{\varphi}(t, \mathbf{x}) = e^{-i\theta/\hbar}\left(\frac{1}{2\sqrt{n_c}}\hat{\rho}_1 - i\frac{\sqrt{\rho}}{\hbar}\hat{\theta}_1\right), \tag{2.9}$$

where $\hat{\rho}_1$, $\hat{\theta}_1$ are real quantum fields which describe the excitations in density and phase, respectively. Inserting the above ansatz in Eq. (2.8), one again obtains a pair of hydrodynamiclike equations for the quantum excitations:

$$\partial_t\hat{\rho}_1 + \frac{1}{m}\nabla\cdot(\rho_1\nabla\theta + \rho\nabla\hat{\theta}_1) = 0, \tag{2.10}$$

$$\partial_t\hat{\theta}_1 + \frac{\nabla\theta\cdot\nabla\hat{\theta}_1}{m} + g(\bar{a})\rho_1 - \frac{\hbar^2}{2m}D_2\hat{\rho}_1 = 0, \tag{2.11}$$

where D_2 represents a second-order differential operator derived from the linearization of the quantum potential [4]. In a long wavelength approximation this can be safely neglected and one can then show (in complete analogy with perfect fluid systems) that the perturbations θ_1 do satisfy a second-order equation of a Klein-Gordon type for a massless scalar field propagating on a curved background geometry described by the metric

$$ds^2 = \sqrt{\frac{\rho}{gm}}[-(c_s^2 - v^2)dt^2 - 2v_i dx^i dt + d\mathbf{x}^2]. \tag{2.12}$$

Here $c_s^2(t, \mathbf{x}) = g\rho(t, \mathbf{x})/m$ is the squared local sound speed of the perturbations and $\mathbf{v}(t, \mathbf{x})$ is the background flow velocity of the BEC introduced above [5,28]. It is then clear that in this long wavelength regime the quasiparticles satisfy a relativistic, phononic dispersion relation $\omega^2 = c_s^2 k^2$ (with ω and k equal, respectively, to the energy and wave number of the quasiparticle). Alternatively, one can adopt an eikonal (short wavelength) approximation and show that the complete dispersion relation is indeed the well-known Bogoliubov dispersion given by $\omega_{\text{Bog}}^2 = c_s^2 k^2 + \hbar k^4/(2m)$. It is evident at this point that in this context the gravitational analogy is valid only in the long wavelength approximation. More specifically, for wavelengths of the order of the healing length $\xi = \hbar/\sqrt{mg\rho}$, when the quartic term becomes comparable to the quadratic one in $\omega_{\text{Bog}}^2(k)$, a geometrical description is no longer available.

B. Scaling solution

Condensates undergoing expansion or contraction as a result of a time-varying confining harmonic potential admit a dynamic generalization to the static TF approximation for the GP equation known as the scaling solution [29,30]. In this case the external potential is of harmonic type with time-varying trapping frequencies:

$$V_{\text{ext}} = \frac{1}{2}\sum_i m\omega_i^2(t)x_i^2. \tag{2.13}$$

Here the density undergoes a simple scaling transformation in each spatial dimension x_i parametrized by the so-called scaling functions $\lambda_i(t)$ as

$$\rho(t, \mathbf{x}) = \frac{\rho_s(x_i/\lambda_i(t))}{\prod_i \lambda_i(t)}, \tag{2.14}$$

where ρ_s is the static TF ground state solution[1]

$$\rho_s = \rho_0\left(1 - \sum_i \tilde{\omega}_i x_i^2\right) \quad \text{if } \sum_i \tilde{\omega}_i x_i^2 < 1, \tag{2.15}$$

$$\rho_s = 0 \quad \text{otherwise,} \tag{2.16}$$

where $\tilde{\omega}_i = m\omega_i^2/2\mu$ (μ being the chemical potential) and ρ_0 is the maximum density at the center of the BEC.

In the static TF approximation the density and chemical potential can be expressed algebraically in terms of the physical parameters as

$$\rho_0 = \frac{\mu}{g(\bar{a})} = \frac{1}{8\pi}\left(\frac{15m^3 N \prod_i \omega_i}{\bar{a}^{3/2}\hbar^3}\right)^{2/5} \tag{2.17}$$

and

$$\mu = \frac{1}{2}\hbar\varpi\left(15N\bar{a}\sqrt{\frac{m\varpi}{\hbar}}\right)^{2/5}, \tag{2.18}$$

respectively, where N is the number of condensed bosons. Here we have introduced the notation $\varpi = (\prod_i \omega_i)^{1/d}$ in d spatial dimensions, the geometric mean of the trapping frequencies. For the phase, the scaling transformation takes the form

$$\theta(t, \mathbf{x}) = \frac{1}{2}m\sum_i x_i^2 \dot{\lambda}_i\lambda_i, \tag{2.19}$$

where $\dot{\ }$ represents the lab time derivative ∂_t.

This scaling induces a background flow velocity profile in the condensate given by

---

[1]Note that the TF approximation is not a good approximation near the boundary of the condensate where the density drops to zero. The condensate boundary, here given by the parabola sharply dropping to zero, in the full solution will be smooth.

$$\mathbf{v}(t, \mathbf{x}) = \frac{\dot{\lambda}(t)}{\lambda(t)} \mathbf{x}. \tag{2.20}$$

With this velocity and the evolution of the density given in (2.14), one can start studying the analogue geometry associated with such a scaling background solution using the metric (2.12).

Of particular experimental interest is the cigar-shaped condensate possessing one elongated dimension ("$\parallel$") and two tightly trapped orthogonal dimensions ("$\perp$"). In what follows, unless otherwise stated, we work with the cigar geometry. Since our main focus will be on such elongated condensates, we list here the following realistic values for the physical parameters describing the cigar BEC:

$$\omega_{\parallel} = 10^2 \text{ Hz}, \qquad \omega_{\perp} = 10^3 \text{ Hz} \tag{2.21}$$

$$m = 1.57 \times 10^{-25} \text{ kg (rubidium 87)} \tag{2.22}$$

$$\bar{a} = 42 \text{ bohr} = 2.221 \times 10^{-9} \text{ m} \tag{2.23}$$

$$N = 10^5. \tag{2.24}$$

These are, respectively, the trapping frequencies, atomic mass, scattering length, and number of condensed atoms. Assuming these numbers, the following derived quantities are obtained:

$$L \approx 5.45 \times 10^{-5} \text{ m} \tag{2.25}$$

$$\mu \approx 5.8 \times 10^{-31} \text{ kg m}^2 \text{ s}^{-2} \approx 5500\hbar \text{ s}^{-1} \tag{2.26}$$

$$\rho_0 \approx 2.9 \times 10^{20} \text{ m}^{-3} \tag{2.27}$$

$$c_{s,0} \approx 2 \text{ mm s}^{-1}, \tag{2.28}$$

corresponding to the transverse condensate size (where, in the TF approximation the density drops to zero), the (static) chemical potential, the maximum condensate density, and the maximum initial sound speed, respectively.

For time-dependent harmonic traps the scaling functions $\lambda_i(t)$ are not free parameters but are constrained to be solutions to the auxiliary equations of motion,

$$\ddot{\lambda}_i(t) + \omega_i^2(t)\lambda_i(t) = \frac{\omega_i^2(0)}{\lambda_i(t)\prod_j \lambda_j(t)}, \tag{2.29}$$

with boundary conditions $\lambda_i(0) = 1$ and $\dot{\lambda}_i(0) = 0$, determined by a self-consistency condition on the dynamics of the expanding condensate [29].

Starting from such a cigar-shaped initial geometry, let us consider the case when the $\parallel$ potential is suddenly switched off while keeping the $\perp$ potentials constant. A similar problem has been studied in [25] and observed in [24], where the authors instead consider a BEC freely expanding in all the three spatial dimensions after completely releasing the trapping potential of an initially cigar-shaped

condensate. In these analyses, due to the expansion in all three dimensions, the density drops very quickly and the gas becomes collisionless signalling the failure of the hydrodynamical description shortly after the release of the trap. In the case we consider here instead, the perpendicular trapping is kept tight and the density drops more slowly and the condensate remains longer in a collisional regime where the spacetime analogy pertains.

In Fig. 1 we show the numerical solution to (2.29) for cigarlike initial geometry after the potential in the $\parallel$ direction is suddenly switched off while keeping the $\perp$ potentials constant. Notice that the tightly constrained $\perp$ dimension in fact pulls even tighter during the expansion in the $\parallel$ dimension as indicated by the decay of the scaling functions $\lambda_{\perp}$. In this way one can understand how the volume of the cigar geometry, scaling as $(\lambda_{\parallel}\lambda_{\perp}^2)^{-1}$, decays much more slowly than in an isotropically expanding BEC which scales as $\lambda_{\parallel}^{-3}$.

C. Validity of the hydrodynamic approximation

As already mentioned above, it is also important to keep track of the hydrodynamical approximation throughout the expansion. Since the quantum pressure scales differently with time than the density, it is of interest to understand whether the hydrodynamic approximation improves or
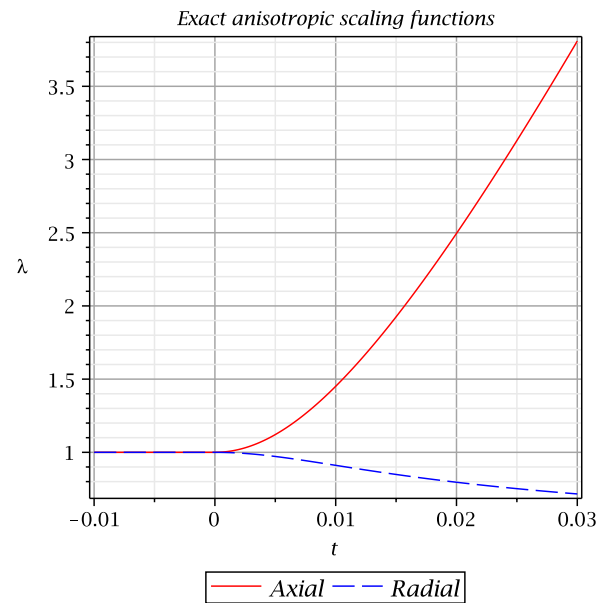

FIG. 1 (color online). The solution of the scaling problem for an anisotropic expansion of an initially cigar-shaped configuration for both the radial/orthogonal (blue-dashed line) and axial/parallel (red-solid line) directions to the axis of release. Note that the scaling function of the direction in which the trapping frequency remains fixed (blue dashed) in fact decreases during the expansion. The parameters used in this solution are $\omega_{\parallel} = 100$ Hz, $\omega_{\perp} = 10^3$ Hz, and a sudden release of the $\parallel$ direction only.
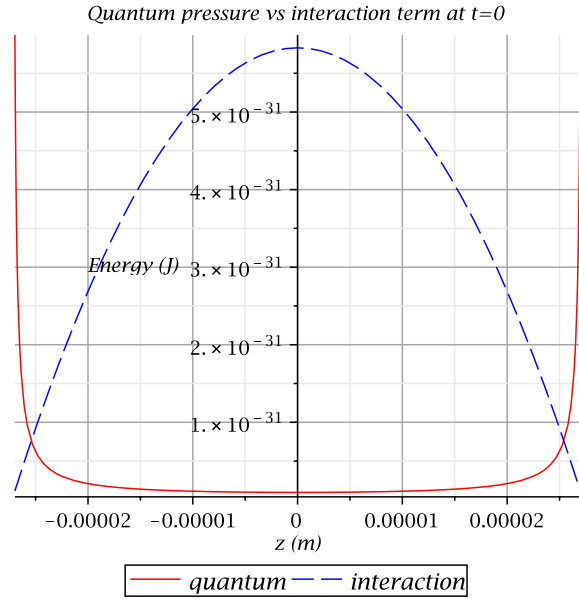
FIG. 2 (color online).   The quantum pressure and interaction energy expressed in Joules as a function of axial distance in meters. Note that the quantum pressure is certainly non-negligible near the boundary of the TF approximate ground state density wave function (at $z \simeq 2.7 \times 10^{-5}$ m).

degrades as the expansion proceeds and, if it loses accuracy, when the approximation breaks down. In Fig. 2 we display the quantum pressure V_{quantum} and interaction $V_{\text{interaction}}$ ($= g\rho$) contributions to GP before the release of the axial trapping potential. In Fig. 3 we display the ratio
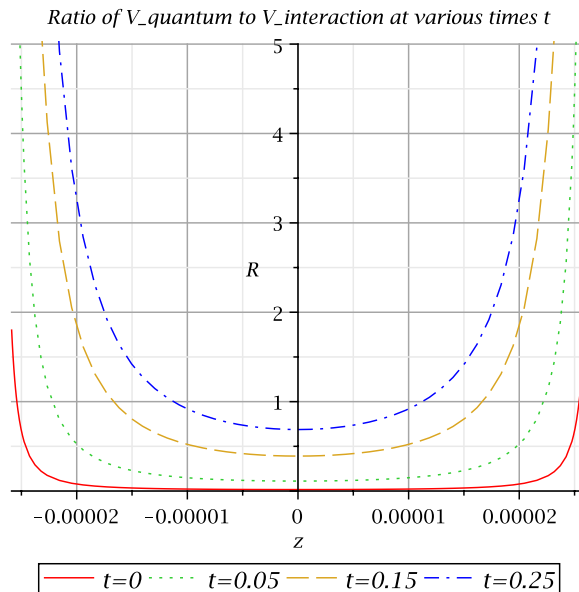

FIG. 3 (color online).   The ratio $R = V_{\text{quantum}}/V_{\text{interaction}}$ as a function of comoving axial position $\tilde{z} = z\lambda_{\parallel}$ at various times t after release of the trapping potential. Note that the axial half length of the condensate at time $t = 0$ (which of course is the comoving length for all times) is $L_z \simeq 2.7 \times 10^{-5}$ m.

$V_{\text{quantum}}/V_{\text{interaction}}$ as a function of comoving axial position $\tilde{z} = z\lambda_{\parallel}$ for four different times after the expansion.

Note that, although there is always a region near the edge of the condensate where the ratio is greater than 1, as time progresses the proportion of the condensate which remains within the hydrodynamical regime gets smaller until approximately $t = 0.25$ s when the quantum pressure becomes important globally in the condensate. The failure of the hydrodynamic approximation near the boundary of the condensate is expected in general since the TF approximation is known to break down on scales on the order of a healing length from the boundary where the density becomes exponentially small. Indeed the true exact solution, being a smooth exponential decay to zero, differs from the TF approximate solution, given in (2.16), near the edge which sharply goes to zero there. Our analysis in the following will be concentrated on the more central part of the condensate where the TF approximation holds.

III. QUANTUM EXCITATIONS

We now intend to consider particle creation associated with the expansion of the condensate and its signature in the correlation structure. Before doing so, however, one might wonder if such expansion is sufficiently rapid to lead to any relevant particle production at all. Also, given that we shall work in the analogue gravity framework, one would also like to be sure that the ostensible excitations can be meaningfully described as phonons rather than having to deal with the complicated issues associated with nonlinear dispersion. We shall discuss these issues first and then introduce the correlation function that will be the subject of our studies.

A. Time scales

Let us now analyze and compare the relevant inverse time scales involved in the problem of an expanding condensate to make an order of magnitude estimate of whether excitation effects can be expected to be observable.

First, there is an intrinsic infrared cutoff given by the size of the condensate. This length scale translates into a frequency ω_s using the (central maximum) sound speed $\omega_s = c_s/(L\lambda(t))$.

Second, there exists an intrinsic ultraviolet cutoff associated with the healing length, the healing frequency $\omega_h = 2\pi c_s/\xi$, where $\xi = \hbar/(mc_s)$ is the healing length. The healing length, as already mentioned, is the length scale at which the quantum potential, neglected in the hydrodynamical approximation, becomes intrinsically comparable with the interaction energy (which is proportional to the density of the condensate and, hence, becomes less relevant at lower densities). This is also the scale at which the Bogoliubov dispersion relation enters in the quadratic regime and, hence, the description in terms of noninteracting phonons breaks down.
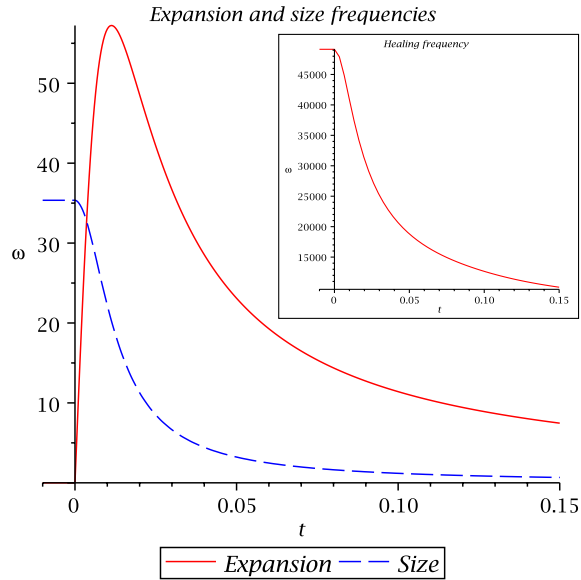
FIG. 4 (color online). A comparison of the relative magnitudes of ω_e and ω_s (red solid and blue dashed, respectively) and with the healing frequency (inset plot) in s^{-1} as a function of time (in s). Note that, for the majority of the duration of the expansion, ω_s is much smaller than the expansion frequency ω_e which is much smaller than the healing frequency. Hence, the bulk of the particle production spectrum lies within the low frequency cutoff provided by the total size of the condensate and the high frequency cutoff provided by the healing length.

Third, there is the characteristic frequency associated with the expansion itself, $\omega_e \approx \dot{\lambda}/\lambda$, which fixes the frequency of the most abundantly created excitations in an expanding condensate. This is generic to any particle creation effect by a time-varying external field (a "dynamical Casimir effect"); see, e.g., [18].

It is of interest to compare these three frequencies in order to test the validity of our approximations and to estimate if the expected excitations are created within the natural ultraviolet and infrared cutoffs. In Fig. 4 we compare these three inverse time scales using the accurate parameters listed above.

We see that indeed there exists a regime in which the typical excitation frequency lies entirely within the natural ultraviolet and infrared cutoff frequencies. Quantitatively this regime begins after about 0.005 s. Let us also note the vastly higher healing frequency representing the UV cutoff for a phononic treatment. This is shown in the smaller subfigure in Fig. 4 for comparison.

Therefore we conclude that there is a viable regime within which the excitations have a phononic (linear) dispersion relation and wavelengths much shorter than the size of the BEC.

B. Wightman functions

The Wightman function $G(x, y) := \langle \phi(x)\phi(y) \rangle$ for a quantum field ϕ is a measure of the correlation between two separate points x and y in spacetime. If the field ϕ were a truly random variable the correlation would be zero everywhere. In general, the equal-time Wightman function for a massless scalar field on a flat $3 + 1$ dimensional Friedmann-Robertson-Walker (FRW) spacetime with scale factor a (which includes Minkowski space as the $a = 1$ special case)[2] only depends on the magnitude of the comoving spatial difference $x = \|\mathbf{x} - \mathbf{y}\|$ and (possibly) on time. This homogeneous function thus is really only a function of these two variables:

$$G(\eta, \mathbf{x}, \mathbf{y}) = \int \frac{d^3k\, d^3k'}{(2\pi)^3} \langle 0|\phi_k \phi_{k'}|0\rangle e^{i(\mathbf{k}\cdot\mathbf{x}+\mathbf{k'}\cdot\mathbf{y})}$$
$$= \int_0^\infty \frac{dk}{2\pi^2} \frac{k}{x} \sin(kx) u_k(\eta) u_k^*(\eta) = G(\eta, x),$$

(3.1)

where $k = \sqrt{\mathbf{k}\cdot\mathbf{k}}$, u_k are the mode-function solutions to $u_k'' + (k^2 - a''/a)u_k = 0$ and $\phi_k = (b_k u_k + b_{-k}^\dagger u_k^*)/(\sqrt{2}a(\eta))$, prime denoting the conformal time derivative ∂_η. In Minkowski spacetime the integral is computed exactly as $G(\eta, x) = \hbar/(4\pi^2 x^2)$ for nonzero x while on the light cone the Wightman function also possesses a singular imaginary part [31]. In $1 + 1$ dimensions the equal-time Wightman function becomes logarithmic and time independent $G(x, y) = -\hbar/4\pi \ln(x - y)^2$ and, owing to the conformal invariance in $1 + 1$ dimensions for the massless scalar field and the conformal flatness of FRW spacetimes, also takes this form in an arbitrary $1 + 1$ FRW background in terms of comoving coordinates and the conformal time variable [2].

IV. CORRELATIONS IN AN ISOTROPICALLY EXPANDING BEC

The main purpose of this section is to gain an intuitive understanding of correlations due to particle production and provide a useful toolbox for the more challenging investigation of the anisotropic scaling solution. In order to do so, we shall study first the ideal case of a homogeneous $3 + 1$D isotropically expanding BEC. In this case, the analogue metric is that of a simple FRW spacetime geometry. We shall choose a scale factor that increases from an initial constant value a_i to a final constant value a_f smoothly as in this case the structure of correlations can be solved for analytically. Our interest in these exactly soluble models derives from the fact that in these systems one can see the appearance in the Wightman function of the characteristic features expected from the creation of particles in a transparent way. Finally, we shall also discuss how to simply interpret such models in terms of a BEC with a varying scattering length.

---

[2]Recall that a FRW spacetime is described by the metric $ds^2 = a^2(\eta)(-d\eta^2 + d\mathbf{x}^2)$ here written in comoving coordinates $\mathbf{x}$ and conformal time η where $a(\eta)$ is a scalar function of time.

A. Exactly soluble expanding spacetime

Written in terms of comoving coordinates $\tilde{x}_i = x_i/\lambda_i(t)$ the metric (2.12) for the scaling solution BEC reads

$$ds^2 = \sqrt{\frac{\rho(t, \mathbf{x})}{gm}}(-c_s^2(t, \mathbf{x})dt^2 + \lambda_i^2(t)d\tilde{x}^{i2}) \qquad (4.1)$$

from which a number of standard representations for a FRW background are easily obtained. The cosmological assumption of homogeneity is satisfied for a BEC in the central region where the density is almost constant. Working in such a central region, ρ and c_s become functions only of t and the metric can be written in standard FRW form as

$$\begin{aligned} ds^2 &= -d\tau^2 + a^2(\tau)d\tilde{\mathbf{x}}^2, \\ \tau(t) &= \int^t dt' \frac{\rho^{3/4}(t')g^{1/4}}{m^{3/4}} \end{aligned} \qquad (4.2)$$

with the scale factor defined by

$$a^2(\tau) = \sqrt{\frac{\rho(\tau)}{gm}}\lambda^2(\tau) \propto \sqrt{\lambda(\tau)}, \qquad (4.3)$$

where we have used the scaling solution $\rho(\eta) = \rho_0/\lambda^3(\eta)$ for the density.

In what follows, however, we will work with the form for the metric given by

$$ds^2 = -a^6(\eta)d\eta^2 + a^2(\eta)d\mathbf{x}^2 \qquad (4.4)$$

which can be obtained from the form (4.2) by the coordinate transformation

$$d\eta = \left(\frac{gm}{\rho_0}\right)^{3/2}\frac{1}{\lambda^{3/2}(\tau)}d\tau. \qquad (4.5)$$

The functional relationship between the scale factor a and the scaling function λ is unchanged in this representation and is given by $a^2(\eta) \propto \sqrt{\lambda(\eta)}$.

Furthermore we will consider the specific form for the scale factor

$$a^4(\eta) = \frac{a_i^4 + a_f^4}{2} + \frac{a_f^4 - a_i^4}{2}\tanh\left(\frac{\eta}{\eta_0}\right), \qquad (4.6)$$

where η_0, a_i, and a_f are constant numerical parameters. Such a metric describes an isotropic homogeneous spacetime with flat spatial sections which expands by a finite amount over a finite time period. This spacetime has been studied previously in the literature, for example, in [18] where it was shown to arise as the analogue geometry experienced by phase perturbations in a BEC with time-varying interaction strength g. In that article the particle content of the initial Minkowski vacuum state after expansion is studied in detail and the observability of the created particles discussed. This spacetime is also studied in [16]

where it is shown to arise as the analogue geometry associated with a ring of trapped ions. A very similar geometry is studied in [22] where, instead of tanh, the authors employ an error function[3] temporal profile for the variable scattering length and the correlation structure is studied semianalytically in the so-called "sudden limit" (which we will discuss later), and numerically in the general case, with the full Bogoliubov spectrum. In [32] the author studies the controlled release of a condensate such that the trapping frequency varies exponentially in time and the associated particle production in terms of the number of particles produced. The separate case of an exponential variation of a time-dependent coupling constant $g(t)$ is also studied as well as the mixed analysis where both the trapping frequency and coupling constant are varied again in terms of the number of particles produced. More recently, in [23] the density correlations in a toroidally shaped BEC with time-varying interaction strength were considered and used to gain information about the character of the quantum squeezing of phononic modes.

The field equation for a massless minimally coupled scalar field ϕ propagating on the background geometry (4.4) decouples into the independent mode equations

$$\partial_\eta^2\phi_k + a^4k^2\phi_k = 0, \qquad (4.7)$$

where $\phi_k = (2\pi)^{3/2}\int d^3\,ke^{-i\mathbf{k}\cdot\mathbf{x}}\phi$ is the kth Fourier component of the field ϕ. For $a(\eta)$ as (4.6) the field equation (4.7) is solved by a rather complicated product of elementary and hypergeometric functions [18]. Conveniently for us, it is not necessary to work explicitly with these cumbersome functions: For each comoving momentum k, the physics of cosmological particle production is contained only in inner products (which we label as α_k and β_k) between two particular solutions ϕ_k^{in} and ϕ_k^{out} to (4.7), solutions which converge, respectively, in the past ($\eta \to -\infty$) and future ($\eta \to \infty$) to plane waves[4] (see, for example, the standard monograph [2]).

Physically, these two particular solutions represent a description of two different vacuum states, |in⟩ and |out⟩, in the two asymptotic regimes where the function $a(\eta)$ becomes constant and the definition of particle state is unambiguous. For example, the quantum state |in⟩ described by the choice ϕ_k^{in} (the vacuum state for $\eta \to -\infty$) is no longer a vacuum (zero particle) state as $\eta \to \infty$ since that state, |out⟩, is described by the mode functions ϕ_k^{out} and in general one has

$$\phi_k^{\text{in}} = \alpha_k\phi_k^{\text{out}} + \beta_k\phi_k^{\text{out}*} \qquad (4.8)$$

---

[3]Recall that the error function is defined as $\text{Erf}(t) \propto \int^t \exp(-x^2)dx$ and smoothly interpolates between constant values.

[4]Specifically α_k is the innerproduct between positive frequency plane waves whereas β_k is the inner product between one positive and one negative frequency plane wave.

with $\beta_k \neq 0$. The spectrum of particle content of the state $|\text{in}\rangle$ at late times in terms of the late time particle states is given by the modulus $|\beta_k|^2$ which has the characteristic bell shape shown in Fig. 5, here shown as a function of the isotropic modulus $k = \sqrt{\mathbf{k} \cdot \mathbf{k}}$ appropriate for the isotropic mode equations (4.7) and hence isotropic coefficients α_k and β_k.

The inner products α_k and β_k (known as Bogoliubov coefficients) are given exactly in this model by the simple expressions

$$\alpha_k = \frac{2\sqrt{AB}}{A + B} \frac{\Gamma(-iA)\Gamma(-iB)}{\Gamma^2(-i(A + B)/2)}$$
$$\beta_k = \frac{-2\sqrt{AB}}{B - A} \frac{\Gamma(-iA)\Gamma(iB)}{\Gamma^2(i(B - A)/2)}, \tag{4.9}$$

where Γ is the Euler function and the dimensionless variables A and B are

$$A = k\eta_0 a_i^2, \qquad B = k\eta_0 a_f^2. \tag{4.10}$$

They are constrained to satisfy $|\alpha_k|^2 - |\beta_k|^2 = 1$ by the constancy of the Klein-Gordon norm of the (unique) solution ϕ written in the two different mode-function bases.

Since the mode functions are simple linear combinations of plane waves long after the expansion has taken place, the equal-time Wightman function there can be written down in a relatively simple way in terms of α_k and β_k alone as

$$G(\eta, x) = \frac{4\pi}{2a_f^2} \int_0^\infty dk \left[\frac{\sin kx}{x}(1 + 2|\beta_k|^2) + I + I^* \right], \tag{4.11}$$

where

$$I = \frac{\sin kx}{x} \alpha_k \beta_k^* e^{-2ika_f^2 \eta}. \tag{4.12}$$

Note again that, given spatial homogeneity and isotropy of the system, here G is a function only of the magnitude of the spatial separation. Of course, such an expression cannot be considered exact for a realistic finite-sized BEC but will break down nearby the boundaries due to finite size effects. Furthermore, in the case of a finite volume cigar-shaped BEC and anisotropic expansion, the expression (4.11) will have to be replaced by a more complicated formula as we shall see in Sec. V.

The expression (4.11) is the sum of three physically distinct terms. The 1 term represents the background zero point fluctuations, the $|\beta_k|^2$ term an enhancement of the background correlations due to particle production, and the terms labeled I and I^* represent additional nontrivial structure propagating on top of the (enhanced) Minkowski-like correlations due to the entanglement between the created pairs of particles. The $I + I^*$ term can be integrated exactly as an unwieldy infinite sum of functions which we do not write down here. In Fig. 6 we plot the result of numerically integrating the contribution from $I + I^*$:
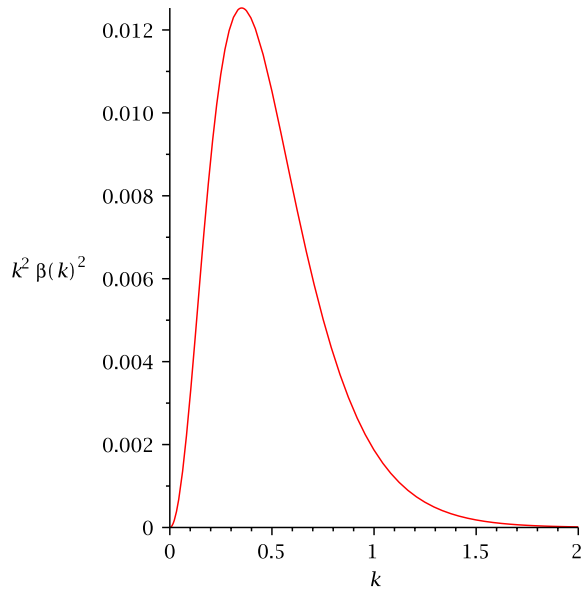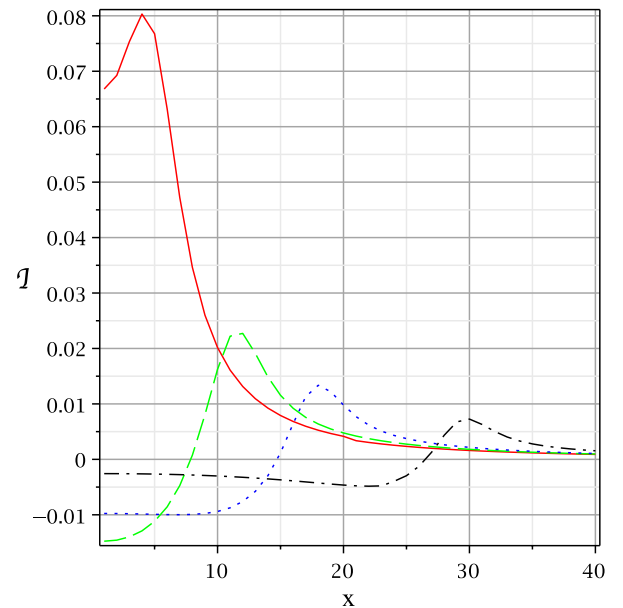

FIG. 5 (color online). The characteristic shape of the spectrum of produced particles in an expanding spacetime described by (4.4), as a function of the modulus $k = \sqrt{\mathbf{k} \cdot \mathbf{k}}$. Recall that the spectrum is proportional to the volume of space $V/2\pi$ as $N_k = Vk^2\beta_k^2/2\pi$ so that what we plot here is in fact particle number density. The peak wave number is fixed by the typical time scale of the expansion $k_{\text{peak}} \propto 1/\eta_0$.

FIG. 6 (color online). The exact numerical integration of (minus) the entanglement contribution to G as a function of point separation x for four successive times $\eta = 0$ (red solid), $\eta = 1$ (green dashed), $\eta = 2$ (blue dotted), and $\eta = 4$ (black dot dashed) for the choice of parameters $a_i^2 = 1$, $a_f^2 = \pi$, and $\eta_0 = 1$.

$$I = \frac{4\pi}{2a_f^2} \int_0^\infty dk(I + I^*) \qquad (4.13)$$

in G for four successive times as a function of separation $x = \|\mathbf{x} - \mathbf{x}'\|$. We see that going backwards in time a bump of correlations merges into the correlation singularity[5] at the origin. The (coordinate) speed of the bump is determined by the final value of the scale factor a_f^2 which in the displayed plot was taken to be π. We note that the bump moves with a velocity of close to 7.5 units per second which is approximately the speed at which two particles moving at speed π units per second would be receding from one another. Note that the coordinate speed is not constrained to be the speed of sound c_s, the coordinate speed in lab variables.

In the next section we show that the essential structure of these correlations is present already in the so-called adiabatic approximation to the integrand $I + I^*$.

1. Adiabatic and sudden approximations

The adiabatic approximation for a mode k is accurate when $k\eta_0 \gg 1$. It is a good approximation for high wave number, or short wavelength modes. These are the modes which feel the expansion as a "slow" process. In the adiabatic limit one can show, from (4.9) and (4.12), that

$$I + I^* \simeq \frac{2}{x} \sin(kx) \sin[k(\Phi - 2a_f^2\eta)]e^{-\pi a_i^2 k\eta_0}, \qquad (4.14)$$

where the phase is given by

$$\Phi = \ln\left(\frac{a_i^2 + a_f^2}{a_f^2 - a_i^2}\right)a_i^2\eta_0 + \ln\left(\frac{a_f^4 - a_i^4}{4a_f^4}\right)a_f^2\eta_0. \qquad (4.15)$$

On the other hand, the sudden approximation is accurate for a given k whenever $k\eta_0 \ll 1$. Hence, it should be a good approximation to the exact result for low wave numbers. In this sudden limit one can similarly show (again from (4.9) and (4.12)) that

$$I + I^* \simeq -\frac{1}{2}\frac{a_f^4 - a_i^4}{a_f^2 a_i^2}\frac{\sin kx}{x}\cos(2ka_f^2\eta) \qquad (4.16)$$

which represents an unbounded contribution to G if assumed accurate over the entire positive k axis (as would be the case in the formal limit $\eta_0 \to 0$). In Fig. 7 we compare the exact, adiabatic approximate and sudden approximate forms of $I + I^*$ for a representative choice of x and η. We note that the adiabatic approximation is accurate almost
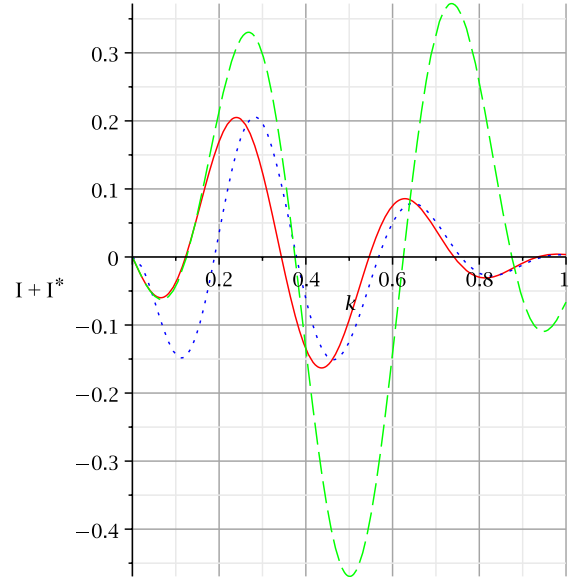

FIG. 7 (color online). A comparison of the exact expression (in red solid) with both the adiabatic approximation (in blue dots) and the sudden approximation (in green dashes) near the turn over region ($k\eta_0 \approx 0.3$) where neither approximation is very accurate. We use the representative values of $t = 2$ and $x = 3$. Note that the sudden approximation is most accurate for small k and the adiabatic for large k. Also note that the adiabatic approximation remains relatively accurate (at least in mimicking the qualitative behavior of the exact function) all the way down to $k = 0$ where the approximation in principle should be poor.

uniformly over all k, even close to the origin, where it is superseded by the sudden approximation while still capturing the qualitative behavior of the $I + I^*$ term.

Integrating the adiabatic approximation $I + I^*$ over k, we observe a "bump" of correlations traveling out from the origin and decaying as displayed in Fig. 8. This is in close agreement with the exact result as shown in Fig. 6. We note that the only feature of the exact result not captured by the adiabatic approximation is the negative "tail" to the bump as it propagates outwards from the origin.

The role of the parameter η_0 is visible in Fig. 9 where we again show the result of integrating the adiabatic approximation[6] to $I + I^*$ for the same values $a_i^2 = 1$ amid $a_f^2 = \pi$ and times $\eta = 0, 2, 4$. One sees that as the rate of expansion increases (as η_0 becomes small) the shape of the bump becomes sharply peaked and that the peak occurs slightly closer to the origin. This is consistent with our intuitive understanding of the bump as arising from propagating particles created during the expansion.

For small η_0 the expansion and hence the particle production takes place over a short time interval. Assume for the purposes of illustration that all the particle production

---

[5]Since we always work under the assumption that the field theory is an effective field theory valid only above a small length scale, for example, the healing length in the case of a BEC, the coincidence singularity does not exist in practice. In the BEC example, higher order contributions to the dispersion relation become non-negligible and in fact dominate at very short length scales resolving the singularity.

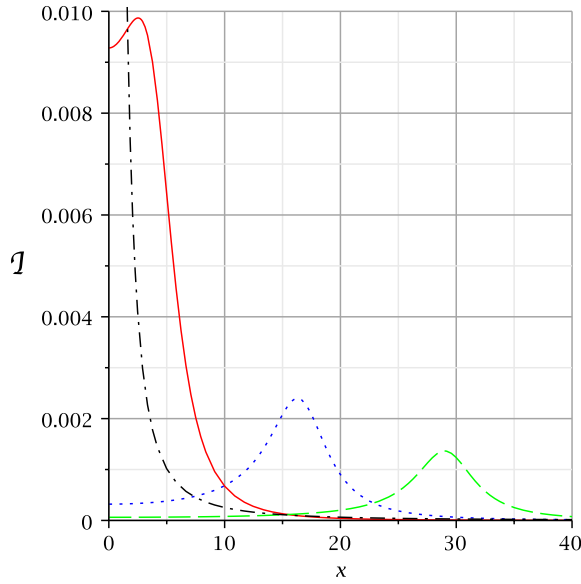[6]For computational reasons we restrict our attention to the adiabatic approximation in this section.

FIG. 8 (color online). The integrated $I + I^*$ contribution to the Wightman function in the adiabatic approximation at three successive times $\eta = 0$ (red solid), $\eta = 2$ (blue dots,) and $\eta = 4$ (green dashes). Note that since the expression (4.11) is only valid after the expansion has taken place (the midpoint of which occurs around $\eta = 0$) the contribution for $t < 0$ are not shown. To make these plots and for comparison with the exact result again we have used the values $a_i^2 = 1$, $a_f^2 = \pi$, and $\eta_0 = 1$. Also plotted (in black dash dotted) is the standard flat spacetime correlations $(4\pi^2 x^2)^{-1}$.

occurs at one point in space, say at X. (Particle production occurs at *every* point but this simplification serves to capture the relevant physical mechanism. Then, two observers at a fixed spatial separation symmetric to X will simultaneously observe a burst of particles passing by. For large η_0 the particle production is spread out over a longer time scale since the scale factor a is changing significantly over a longer period and, hence, the observers will see a more diffuse burst of particles. In this way it is not surprising that attempting to integrate the sudden approximate solution over all k (that is, in the formal $\eta_0 \rightarrow 0$ limit) one finds a propagating singularity at approximately $x = 2a_f^2 \eta$ as can be inferred from the structure of (4.16).

2. Varying scattering length interpretation

As mentioned at the beginning of this section, the metric (4.4) can be used to describe phase perturbations in a BEC with a time-dependent scattering length $\bar{a}(t)$ [and hence coupling parameter $g(t)$ and sound speed c_s] as discussed in the article [18]. In such varying scattering length models, one works in a homogeneous approximation where the background condensate density ρ is assumed constant and the flow velocity **v** everywhere zero. The FRW scale factor (which we temporarily write as a_s for clarity) is related to the scattering length $\bar{a}$ by

$$a_s(\eta) = \left(\frac{\rho}{4\pi\hbar^2}\right)^{1/4} \frac{1}{\bar{a}^{1/4}(\eta)}. \tag{4.17}$$

Hence, a decrease in the scattering length corresponds to an expansion of the FRW spacetime and vice versa. In [18] the authors use this form for the metric and also the tanh scale factor profile (4.6) described above.

We interpret our result in this context as a propagating bump of correlations when the scattering length is varied according to

$$\bar{a}(\eta) = \frac{\rho}{4\pi\hbar^2}\left(\frac{a_i^4 + a_f^4}{2} + \frac{a_f^4 - a_i^4}{2}\tanh\left(\frac{\eta}{\tau_0}\right)\right)^{-1}. \tag{4.18}$$

Note that this time dependence is not determined by any internal dynamics of the BEC but instead is a free experimental choice. This is in contrast with the expanding BEC case where the time-dependent parameter, the scaling function λ, is determined by the internal dynamics of the BEC.

V. AXIAL CORRELATIONS IN AN EXPANDING ELONGATED CONDENSATE

We shall now consider the experimentally relevant case of an anisotropic harmonically trapped BEC, where the trap is released only along the z dimension. The radial trapping is taken to be sufficiently tight to bring the radial dimension of the condensate within the order of a healing length. Because of this small radial size, radial and angular phononic modes necessarily would oscillate on length scales shorter than the minimal healing length and are hence absent and do not contribute to the action for density fluctuations. In other words, in order for a mode of the density fluctuation field to satisfy the ultraviolet band limitation, it must necessarily not contain any nonzero radial or angular frequencies.

The condensate is described by a $1 + 1$D density profile and single scaling function [33] which we write as $\lambda(t) := \lambda_z(t)$. The simple form of the scaling solution in this case allows us to separate the variables in the effectively $1 + 1$D background velocity as $c_s(t, z) = \tilde{c}(\tilde{z})/\sqrt{\lambda(t)}$, where $\tilde{c} = c_s\sqrt{1 - \tilde{\omega}_z \tilde{z}^2}$ and $\tilde{\omega}_z$ was defined in Sec. II B.

Let us now introduce new coordinates through the exact differential expressions

$$dT = \frac{dt}{\lambda^{3/2}\lambda_\perp}, \qquad dZ = \frac{d\tilde{z}}{\tilde{c}(\tilde{z})}. \tag{5.1}$$

Then the metric (4.1) is written as

$$ds^2 = \sqrt{\frac{\rho_s}{gm}}\lambda^2\tilde{c}^2\left\{-dT^2 + dZ^2 + \left(\frac{\lambda_\perp}{\lambda\tilde{c}}\right)^2 d\tilde{r}^2\right.$$
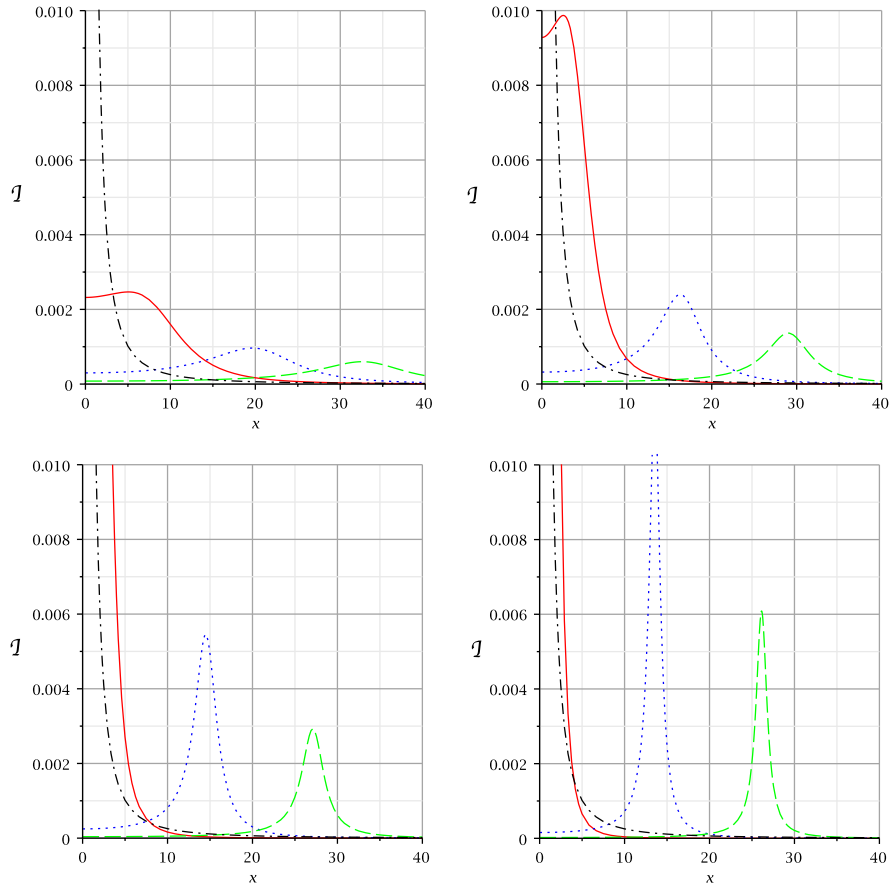$$\left. + \left(\frac{\tilde{r}\lambda_\perp}{\lambda\tilde{c}}\right)^2 d\theta^2\right\}. \tag{5.2}$$

FIG. 9 (color online).   Comparison of the bump structure of correlations for three different values of the parameter $\eta_0 = 2$, 1, $1/2$, and $1/4$ (from top left to bottom right) at three different times $\eta = 0$ (red solid), $\eta = 2$ (blue dots), and $\eta = 4$ (green dashes). Also plotted (in black dash dotted) is the standard flat spacetime correlations for comparison.

Relabeling $\phi := \hat{\theta}_1$ the action for phase perturbations written in these coordinates is

$$
\begin{aligned}
S &= -\frac{1}{2} \int d^4 x \sqrt{\mathbf{g}} g^{\mu\nu} \partial_\mu \phi \partial_\nu \phi \\
&= -\frac{1}{2} \int dT dZ \Omega(T, Z)[-(\partial_T \phi)^2 + (\partial_Z \phi)^2] \\
&\quad + \mathcal{O}(\partial_r \phi) + \mathcal{O}(\partial_\theta \phi),
\end{aligned} \tag{5.3}
$$

where

$$
\Omega = \sqrt{\frac{\rho_s}{gm}} A_\perp \tag{5.4}
$$

and $A_\perp$ is the cross sectional area of the condensate. The action (5.3) has been written up to terms involving the radial and angular derivatives of the field ϕ which we discard as mentioned above.

Explicit formulas for the function Ω in terms of the lab coordinates (t, z) are obtained by assuming a

$$
\Omega(t, z) = \Omega_0 \frac{1}{\sqrt{\lambda}} \left(1 - \tilde{\omega}_\| \frac{z^2}{\lambda^2}\right)^{1/2}, \tag{5.5}
$$

where

$$
\Omega_0 = \frac{2\pi A_\perp}{g} \left(\frac{\mu}{m}\right)^{3/2}. \tag{5.6}
$$

Here it is understood that $\Omega(t, z)$ has support only on the extent of the condensate and is zero if the right-hand side becomes negative.

The field equation for the action (5.3) is

$$
-\partial_T(\Omega \partial_T \phi) + \partial_Z(\Omega \partial_Z \phi) = 0 \tag{5.7}
$$

and we shall work with this field equation in what follows.

A. Conformal symmetry approximation

As a zeroth order attempt at uncovering a signature of "cosmological" particle creation in the Wightman function, one might be tempted to discard derivatives of the function Ω. Under such an approximation the field equation reduces to the flat $1 + 1$ dimensional wave equation for the scaled field $\tilde{\phi} = \Omega \phi$ whose solutions are simple exponentials. The Wightman function for the phase field ϕ is then simply related to the standard Green function as

$$\langle \phi(T,Z)\phi(T',Z')\rangle = \frac{\langle \tilde{\phi}(T,Z)\tilde{\phi}(T',Z')\rangle}{\Omega(T,Z)\Omega(T',Z')}$$

$$= -\frac{\hbar}{4\pi}\frac{\ln[\Delta x^+ \Delta x^-]}{\Omega(T,Z)\Omega(T',Z')}, \qquad (5.8)$$

where $x^\pm$ are the characteristic null coordinates. However, this is immediately seen to be too strong an approximation to capture any particle production effects. In fact, the above correlator can be easily plotted as in Fig. 10, which shows no sign of the typical transient propagating overcorrelation feature normally associated with particle production (see Sec. IVA).

This observation seems to be at odds with several results found in some literature concerning the correlation structure in the case of Hawking radiation. For example, in [8,9] an analogous calculation is performed to the one here, dimensionally reducing a 3 + 1D BEC dynamical problem down to one in 1 + 1D in the case of an acoustic black hole background geometry for phase perturbations. The important point for the current discussion is that the authors of [8,9] in fact do observe numerically a signature of created Hawking quanta in the same approximation which neglects all the derivatives of the function Ω. However, there the nontrivial "cross-horizon" correlations are contained entirely to the relationship between the lab coordinates x and t and the null coordinates $x^\pm$. Indeed also in [10] these correlations across the horizon are demonstrated for an explicitly 1 + 1D black hole geometry[7] which, being conformally flat, possesses the standard logarithmic functional form for the correlator. Again the Hawking signal is contained exclusively in the relationship between the null and lab coordinate functions.

The reason for this discrepancy is rooted in the rather different causal structure of the black hole and cosmological analogue spacetimes and in the inherently different natures of the associated particle creation processes. In the black hole spacetime the presence of the acoustic horizon is associated to an ergoregion which allows for negative energy states (with respect to an asymptotic observer) and these states in turn allow for the stationary Hawking flux on the black hole static spacetime. In the case of the cosmological analogue geometry there is not such an ergoregion and particle production is permitted only as a result of the time dependence of the geometry. This time dependence is fully encoded in the conformal factor describing the difference from Minkowski space of the analogue geometry. It is then clear that, when one introduces an approximation which induces a conformal

---

[7]Note the difference between the analyses of [10] and [8,9]: whereas [10] works exclusively with the 1 + 1D conformally flat geometry and the minimally coupled field, the 1 + 1D action of [8,9] arises from a dimensional reduction of a 3 + 1D model. This dimensional reduction is encoded in the 1 + 1D dynamics by the factor Ω which renders the field nonminimally coupled to the geometry.

Field correlator during eternal expansion as a function of time
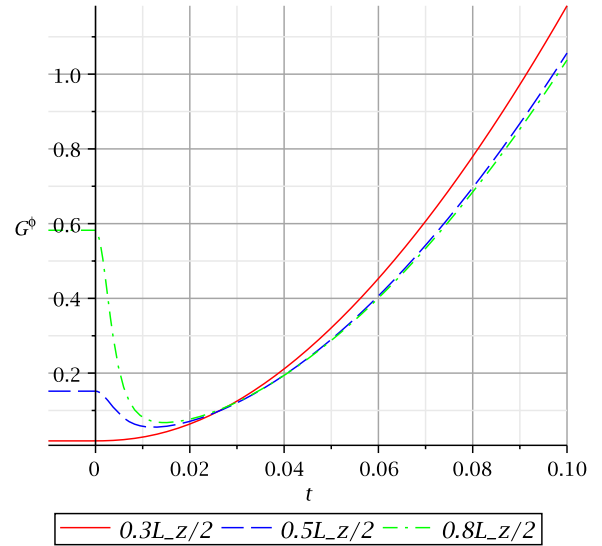

FIG. 10 (color online). The field (phase) correlations G^ϕ as a function of time t for three different fixed laboratory spatial separations $0.2L_z$, $0.5L_z/2$, and $0.8L_z/2$.

symmetry in the field equation, no particle production can take place.

B. Spatially homogeneous $\Omega(Z)$ approximation

As discussed above, the approximation in which we discard both temporal and spatial derivatives of Ω is too strong to capture the physics of particle creation in the 1 + 1 dimensional massless case. However, we shall now argue that it is sufficient to keep the T derivatives while neglecting the Z derivatives of Ω to observe to particle creation signal.

First, since the relationship between Z and the comoving lab coordinate $\tilde{z}$ is given by integrating (5.1) to

$$Z(\tilde{z}) = \frac{\sqrt{2}}{\omega_z}\arcsin\left(\sqrt{\frac{m\omega_z^2}{2\mu}}\tilde{z}\right), \qquad (5.9)$$

we see that $\partial_Z\Omega$ is naturally suppressed. One has

$$\partial_Z\Omega = \frac{\partial z}{\partial Z}\partial_z\Omega, \qquad (5.10)$$

where the first factor $\partial z/\partial Z$ is naturally small near the boundary (but still within the region in which the TF approximation remains valid) and the second factor $\partial_z\Omega$ is naturally small in the central region where the condensate density is almost constant. Therefore, the factor $\partial_Z\Omega$ is naturally small everywhere on the condensate.

No such natural cancellation is available for $\partial_T\Omega$ since $\partial t/\partial T = \lambda^{3/2}$, which is not naturally a small factor. Hence, in what follows we will keep only T derivatives of Ω and discard the Z derivatives.

Note that this approximation is not the same as assuming Ω to be constant in lab coordinates, the difference being in the extra factor of dz/dZ which suppresses ∂_Z at the boundary of the condensate. An important feature of our analysis here is the inclusion of the effects of nonconstant density and finite condensate size.

1. Phase-phase correlations

Consider, then, (5.7) and assume Ω is a function only of the variable T. Then (5.7) is written

$$- \partial_T^2 \phi - \frac{\Omega_{,T}}{\Omega} \partial_T \phi + \partial_Z^2 \phi. \qquad (5.11)$$

Let η be defined by the differential expression $dT = \Omega d\eta$. Then (5.11) separates to

$$\partial_\eta^2 \phi_k + \Omega^2(\eta) k^2 \phi_k = 0, \qquad (5.12)$$

where $\phi_k = (2\pi)^{-1} \int_L dZ \phi e^{-ikZ}$ is the kth Fourier component of the function ϕ and L is the Z size of the condensate.

Since we work in the compact region L, inverse Fourier integrals will be replaced by discrete Fourier series in this section. Hence k in (5.12) is constrained to satisfy $k = 2n\pi/L$ after choosing the boundary conditions $\phi(-L/2) = \phi(L/2) = 0$.

Such an equation of motion can be solved exactly, as we did in the previous section whenever Ω^2 is contained in the three parameter family of functions

$$\mathcal{S} := \left\{ \frac{a_i^2 + a_f^2}{2} + \frac{a_f^2 - a_i^2}{2} \tanh\left(\frac{\eta}{\eta_0}\right) \,\Big|\, a_i, a_f, \eta_0 \in \mathbb{R} \right\}. \qquad (5.13)$$

Our strategy here will be to make use of the available exact solutions and try to find a suitable element in $\mathcal{S}$ labeled by (a_i, a_f, η_0) which most accurately reproduces the exact function Ω associated with free expansion of the BEC. We will see that such a class of functions is indeed appropriate for an approximation to the free expansion case with the key benefit of a description in terms of asymptotic particle states.

An alternative way to think about this approximation methodology is that one is studying the correlations in a BEC which really has this particular form for the function Ω. As will be discussed later, there is a rather direct link between Ω and the scaling functions λ. In fact from (5.5) we see that $\Omega^2 \propto \lambda^{-1}$ so that $\Omega^2 \in \mathcal{S}$ are models for "finite expansion" condensates (or "finite contraction" depending on the relative magnitudes of a_i and a_f). Such finite expansion (contraction) condensates are achievable in the lab with a suitable ramp-down or ramp-up trapping potential (see Sec. V C). Note that the finite expansion case qualitatively differs from the free expansion case only in the future asymptotically static region.

Recall from Fig. 4 that the typical frequency of produced particles during expansion is $\dot{\lambda}(t)/\lambda(t)$ which converges to zero at late times for a linear expansion $\lambda(t) \propto t$. For this reason we expect all the particle production in the infinite expansion case to occur only during the "accelerating" phase and that all of the interesting physics to have ceased by the time the scaling function becomes a linear function of time which occurs at late time. In this way we expect the finite expansion approximation to free expansion to capture the relevant physics neglecting only the irrelevant linear phase of expansion at late times.

The strategy to understand particle production effects in the correlator is as follows. We choose the quantum state to be $|\text{in}\rangle$ (and since we work in the Heisenberg picture the system remains in this state for all time) and express our results in the $\eta \to \infty$ limit in terms of the number eigenstates of the asymptotic Hamiltonian which are the physical particle states in that region.

Let us now move back to the θ notation for the phase perturbation field. The field operator is written in $1 + 1D$ as the sum

$$\theta = \sum_k b_k f_k + b_k^\dagger f_k^*, \qquad (5.14)$$

where the functions f_k satisfy the equation of motion (5.12) and are proportional to plane waves in the past and linear combinations of plane waves in the future as

$$f_k(\eta \to \infty, Z) \propto \sin kZ(\alpha_k e^{-i\omega_k \eta} + \beta_k e^{i\omega_k \eta}). \qquad (5.15)$$

The normalization for the functions f_k is not determined by (5.12) but instead by the consistency between the commutation relations for b_k with the commutation relations between the field operator θ and ρ, the density perturbation field. To fix this normalization we will use the commutator $[\theta(Z), \partial_t \theta(Z')]$. In $3 + 1D$ in the TF approximation with zero background velocity flow in the BEC, one has $\rho = -\partial_t \theta/g$ as well as the fundamental commutator $[\theta(x), \rho(x')] = -i\hbar \delta^3(x, x')$ implying $[\theta(x), \partial_t \theta(x')] = i\hbar g \delta^3(x, x')$. Recall that we assume the perturbation field to be constant over the cross sectional area of the condensate (which was related to the existence of a UV cutoff at the healing length). Hence, integrating this commutator we get for the $1 + 1D$ phase field an extra factor of the area from $\rho^{(3+1)} A_\perp = \rho^{(1+1)}$ and, hence,

$$[\theta(x), \partial_t \theta(x')] = \frac{i\hbar g}{A_\perp} \delta(x, x'). \qquad (5.16)$$

Further, expressing this commutator in Z coordinates we recall that the conjugate momentum is a density of weight one whereas the field θ is a scalar so that one picks up a factor of the Jacobian under a coordinate transformation

$$[\theta(Z), \partial_t \theta(Z')] = [\theta(x), \partial_t \theta(x')] \frac{dZ}{dx}. \qquad (5.17)$$

Therefore

$$[\theta(Z), \partial_t \theta(Z')] = \frac{i\hbar g \lambda_f}{c_{s,0} A_\perp} \delta(Z, Z'), \quad (5.18)$$

where $c_{s,0}$ is the initial sound velocity (which appears as a result of the use of $\tilde{c}_s$ instead of c_s in the definition of the coordinate Z) and λ_f is the final value of the scale factor λ (which comes from the relationship between comoving $\tilde{x}$ and lab x). The dispersion relation is easily computed to be $\omega_k^2 = \Omega^2 k^2 \rightarrow a_f^2 k^2$ using the metric in (η, Z) coordinates. Hence, we arrive at the expression

$$\frac{ig\hbar \lambda_f}{c_{s,0} A_\perp} \delta(Z, Z') = [\theta(Z), \partial_t \theta(Z')]$$

$$= \sum_{k,k'} [b_k, b_k^\dagger](f_k \partial_t f_k^* - f_k^* \partial_t f_k) \quad (5.19)$$

which relates the commutators and the Wronskian for the mode functions allowing us to fix the normalization factor.

For a Fock space (particle) representation, we require $[b_k, b_{k'}^\dagger] = \delta_{kk'}$. Hence, we arrive at the Wronskian constraint on the mode functions

$$\sum_k (f_k \partial_t f_{k'}^* - f_k^* \partial_t f_{k'}) = \frac{ig\hbar \lambda_f}{c_{s,0} A_\perp} \delta(Z, Z'). \quad (5.20)$$

In order to take the laboratory time derivatives above we require the relationship between t and η. We have

$$d\eta = \frac{dT}{\Omega} = \frac{1}{\Omega} \frac{dt}{\lambda^{3/2}} = \frac{\Omega^2}{\tilde{\Omega}_0^3} dt, \quad (5.21)$$

where we have first transformed to the variable T using $dT = \Omega d\eta$ and consequently to t using (5.1), expressing the result in terms of Ω alone. Ω and λ are related by (5.5) as $\Omega = \tilde{\Omega}_0 / \sqrt{\lambda}$, where $\tilde{\Omega}_0$ is the spatial part of Ω, numerically (for $A_\perp = \xi^2$, a healing length squared) $\tilde{\Omega}_0 \approx 1.4 \times 10^{37}$. Then

$$dt = \frac{\tilde{\Omega}_0^3}{\Omega^2} d\eta = \frac{\tilde{\Omega}_0^3 d\eta}{\frac{a_i^2 + a_f^2}{2} + \frac{a_f^2 - a_i^2}{2} \tanh(\frac{\eta}{\eta_0})}. \quad (5.22)$$

Now, we wish to approximate the free expansion scale factor shown in Fig. 1 for approximately the first $t = 0.15$ s. This choice of the approximation region is motivated by two constraints: First, after about $t = 0.15$ s, a large proportion of the condensate no longer is described accurately by a TF approximation as can be seen in Fig. 3; second, the natural shape of the exact free expansion scaling function is less accurately fit by the tanh functions we use here over longer time periods since the scaling function enters a linear regime at late times.

Over this $t = 0.15$ s time interval the scaling function λ increases from $\lambda_i = 1$ to approximately $\lambda_f = 25$. Since $\Omega = \tilde{\Omega}_0^{-1}/\sqrt{\lambda}$ we see that the variable Ω must *decrease* from $\tilde{\Omega}_0$ to $\tilde{\Omega}_0/5$. Therefore we must have $a_f = a_i/5$. Hence, by (5.22) we have the asymptotic relations between the time variables

$$t(\eta) = \begin{cases} \lambda_i \tilde{\Omega}_0 \eta, & \text{for } t \rightarrow -\infty \\ \lambda_f \tilde{\Omega}_0 \eta, & \text{for } t \rightarrow \infty, \end{cases} \quad (5.23)$$

where the function $t(\eta)$, obtained by integrating exactly the differential expression (5.22), varies smoothly between these two constant asymptotes in the intermediate region. Taking the average gradient in the intermediate region for $t(\eta)$, we see that a t interval of 0.15 s corresponds to an η interval of approximately $12 \times \tilde{\Omega}_0 \approx 8.2 \times 10^{-40}$ (in units of $[\Omega^{-1}]$ s or $[\text{energy}] \cdot [\text{time}]^2$). Therefore, we require the function $\Omega(\eta)$ to vary over this time scale between the initial and final values a_i and a_f. That is we should choose

$$\eta_0 \approx 8.2 \times 10^{-40} [\text{energy}] \cdot [\text{time}]^2. \quad (5.24)$$

With these choices one finds that $\omega_k \eta = kt/\lambda_f^{3/2}$.

For the unnormalized f_k we have

$$\sum_k (f_k \partial_t f_k^* - f_k^* \partial_t f_k) = 2 \sum_k \frac{ik}{\lambda_f^{3/2}} \sin kZ \sin kZ'. \quad (5.25)$$

Scaling the functions f_k as

$$\tilde{f}_k = \sqrt{\frac{\lambda_f^{3/2} \hbar g}{\text{Vol} A_\perp c_s^i k}} f_k, \quad (5.26)$$

where Vol is the axial Z length of the condensate (which has the dimension of a time), the Wronskian provides the correct numerical and functional form for the commutator.

Hence, the correctly normalized mode functions are given by

$$f_k = \frac{\sqrt{\lambda_f^{3/2} \hbar g}}{\sqrt{c_s^i A_\perp \text{Vol}}} \frac{\sin(kZ)}{k} e^{-ikt/\lambda_f^{3/2}}. \quad (5.27)$$

Here we have transformed back to lab t coordinates in which we take the time derivatives.

In $1 + 1$D at late times the equal-time Wightman function is written in terms of α_k and β_k in a very similar way to the $3 + 1$D example above in terms of the discrete (and inhomogeneous) Fourier series,

$$G^\theta(\eta, Z, Z') = N \sum_{n=1}^\infty \frac{1}{n} \sin(k_n Z) \sin(k_n Z')(1 + 2|\beta_{k_n}|^2$$
$$+ 2 \operatorname{Re} \alpha_{k_n} \beta_{k_n}^* e^{-2ik_n a_f \eta}), \quad (5.28)$$

where the normalization factor N is given by

$$N = \frac{\lambda_f^{3/2} \hbar g}{A_\perp c_{s,0} \pi}. \quad (5.29)$$

Taking symmetrically spaced points from the center of the condensate, the transient time-dependent contribution is given by

$$I = N \sum_{n=1}^{\infty} \frac{1}{n} \sin\left[n\pi\left(1 + \frac{2Z}{L}\right)\right]$$

$$\times \sin\left[n\pi\left(1 - \frac{2Z}{L}\right)\right] 2\,\mathrm{Re}\,\alpha_{k_n}\beta_{k_n}^* \, e^{-2ik_n a_f \eta} \quad (5.30)$$

and is easily computed as a truncated sum.

With the choices made above for the parameters a_i, a_f, and η_0, we find the entanglement structure shown in Fig. 11. The time scales of the propagating bump are understood in terms of the crossing time for the massless modes: After the expansion the sound speed has decreased to one-fifth its initial value $c_s/5$ due to the dilution of the BEC gas [$\lambda(t \to \infty) = 25$]. The size of the condensate has increased by a factor of 25 so the crossing time increases by a factor of 125. Initially with an axial length of $L_z = 5 \times 10^{-5}$ m and $c_s = 2 \times 10^{-3}$ ms^{-1} the crossing time is $t_{\mathrm{crossing}} = 5 \times 10^{-2}$ s which increases to the order of seconds after expansion. (Note again as in the $3 + 1$D case, that the entanglement propagation speed is twice the sound speed since it represents pairs of phonons traveling in opposite directions.) This is a slight overestimation since the sound speed actually decreases from a maximum at the center of the condensate to zero at the edge. However, we have neglected this slowing in the analysis. This order of magnitude estimate is confirmed in the plot of Fig. 11.

In Fig. 12 we show also the integrated contributions from the "1" and "$|\beta_k|^2$" terms in the integrand, in the same units as Fig. 11. We note that the magnitude of the bump structure is in general much larger than the background ("1") and enhancement ("$|\beta_k|^2$") contributions. This is expected since the produced particles propagate from small distances where there is a high intrinsic correlation to long distances where the natural background fluctuations are no longer correlated.
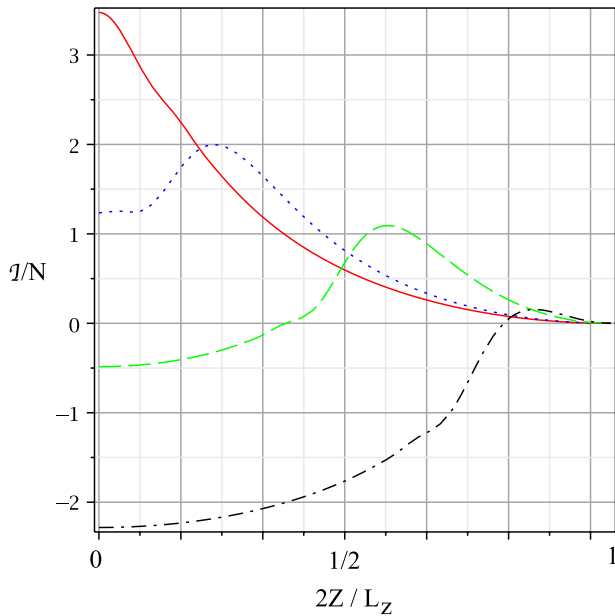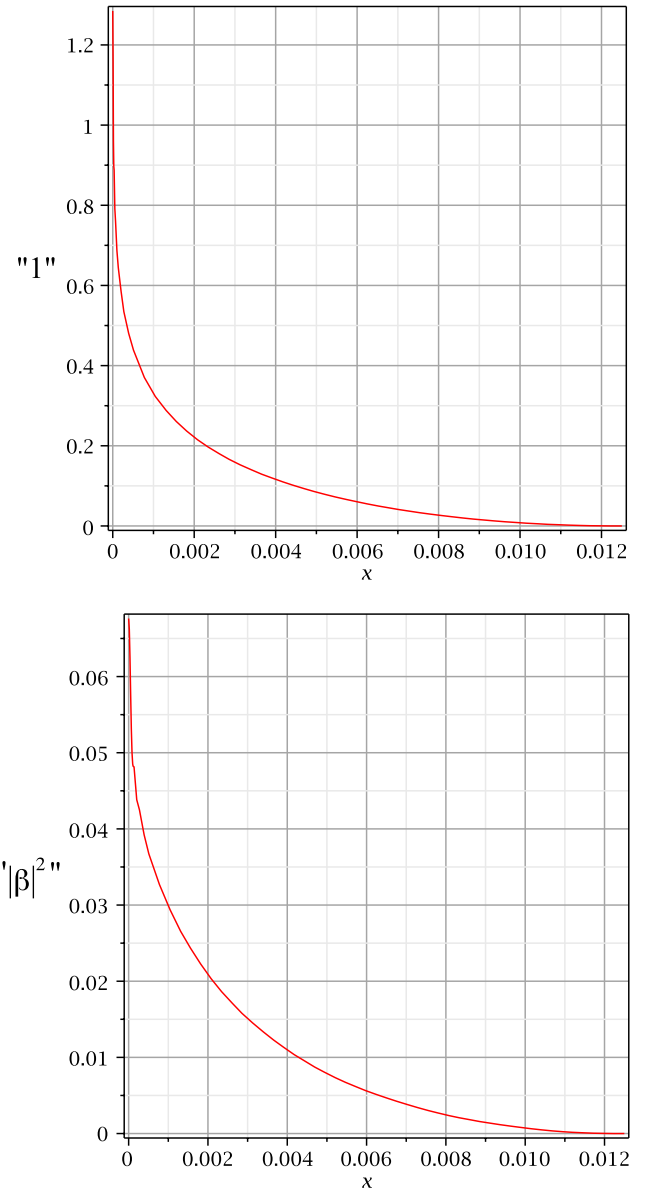

FIG. 11 (color online).   The bump of correlations propagating outwards from the center of the BEC cloud. The curves are for $t = 0$ s (red solid), $t = 0.3$ s (blue dotted), $t = 0.8$ s (green dashed), and $t = 1.2$ s (black dash dotted) Here we plot the truncated sum up to the first 90 terms. The horizontal axis of this plot is the fraction of the half length $L_z/2$ of the condensate after expansion. The vertical axis is the integrated contribution Ent in units of the normalization factor N.

FIG. 12 (color online).   The contributions to the phase Wightman function from the "1" and "$|\beta_k|^2$" terms in (5.28) truncated to the first 200 term of the series. Such a truncation serves as an ultraviolet regulator on the correlation singularity at the origin of the "1" background contribution. No such UV divergence is present in the "$|\beta_k|^2$" contribution.
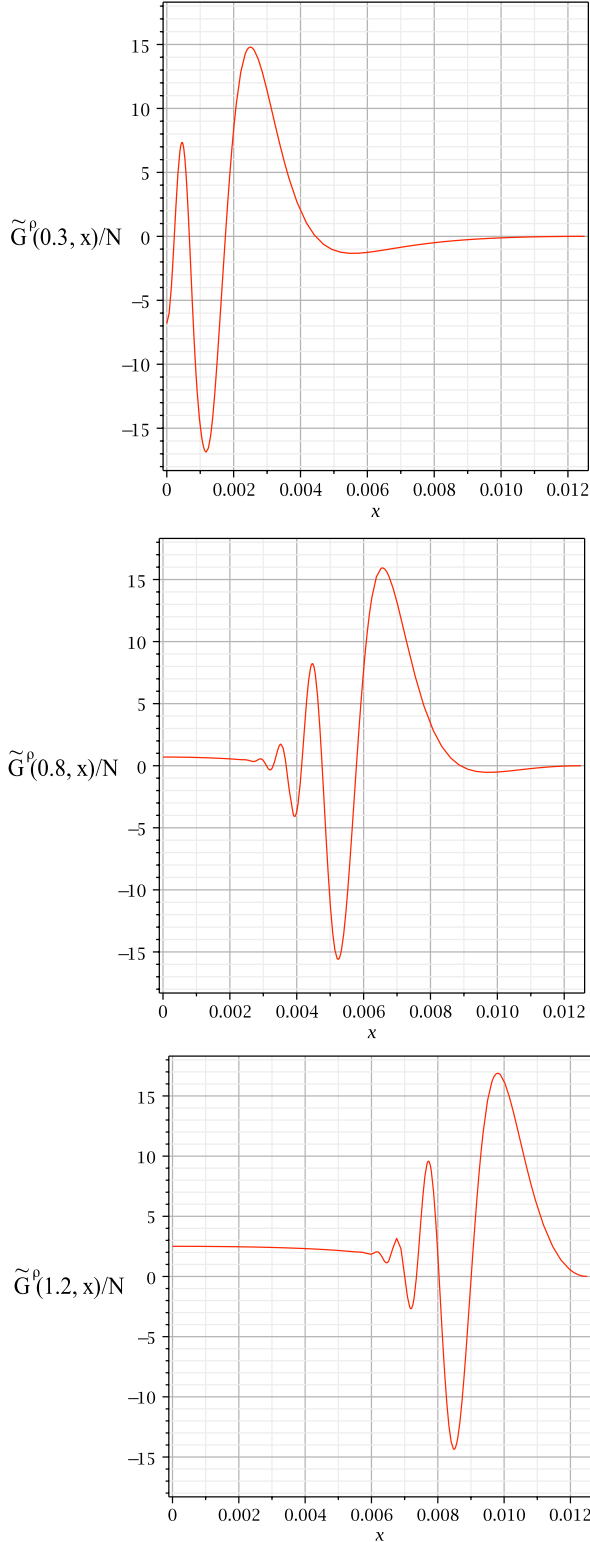
FIG. 13 (color online).   The density correlation function after expansion has taken place, for the finite expansion case, in units of $N \times A_\perp^2/g^2$. The curves from top to bottom correspond to $t = 0.3$ s, $t = 0.8$ s, and $t = 1.2$ s after the onset of expansion (which we take, as described above, to last for 0.15 s).

2. Density-density correlations

Experimentally, although there are proposals to directly measure the phase correlations, the density correlations are those of major observational interest. Again, in the TF approximation the density field is written in terms of the phase as

$$\rho^{(3+1)} = -\frac{1}{g}\partial_t\theta - \frac{1}{g}v_z\partial_z\theta. \tag{5.31}$$

The $1 + 1$D density is related to the $3 + 1$D density by $\rho^{(3+1)} = \rho^{(1+1)}A_\perp$, where $A_\perp$ is the cross sectional area of the condensate (which we assume constant). Then the density correlator is derived according to

$$G^\rho(z, z') = \lim_{t \to t'}\mathcal{D}G^\theta(t, t', z, z'), \tag{5.32}$$

where we define the differential operator $\mathcal{D}$ as

$$\mathcal{D} = \frac{A_\perp^2}{g^2}(\partial_t + v_z\partial_z)(\partial_{t'} + v_{z'}\partial_{z'}). \tag{5.33}$$

In the $1 + 1$D finite expansion case, $\mathcal{D}$ reduces to simply the time derivative since $v_z = 0$ after the expansion has finished. In Fig. 13 we plot the normalized density correlator $\tilde{G}^\rho(t, z, z') := G^\rho(t, z, z')/(\rho^{(1+1)})^2$ for symmetrically placed points z, z' about the middle of the condensate in units of $N \times A_\perp^2/g^2$. We note again the propagating structure but of a slightly more complicated shape to the phase correlation bump.

C. Finite expansion of an elongated BEC

The availability of an asymptotically static regime in the future is a necessary ingredient for the application of the Bogoliubov formalism. As discussed above there are two ways to use the tools contained in that formalism to understand a system which does not possess such a future static regime such as the case of indefinite expansion of a released BEC. Either one considers the finite expansion as a theoretical approximation to the "true" unconstrained expansion case, as shown in Fig. 14, or alternatively one can imagine actually performing a finite expansion experiment in the lab with a condensate which is at first released and consequently "caught" after a finite expansion. Above we have essentially been discussing the first interpretation. Here we briefly discuss the second.

In order for $\lambda(t)$ to follow the correct step up profile with a future nondynamical region, one might expect a simple two level potential would suffice. However, the equations of motion (2.29) for the scaling function admit oscillating solutions so that in order to arrive at a static condensate in the asymptotic future a rather finely tuned potential is necessary.

Again assuming the constancy of the radial scaling functions during the axial expansion we have for the trapping frequency
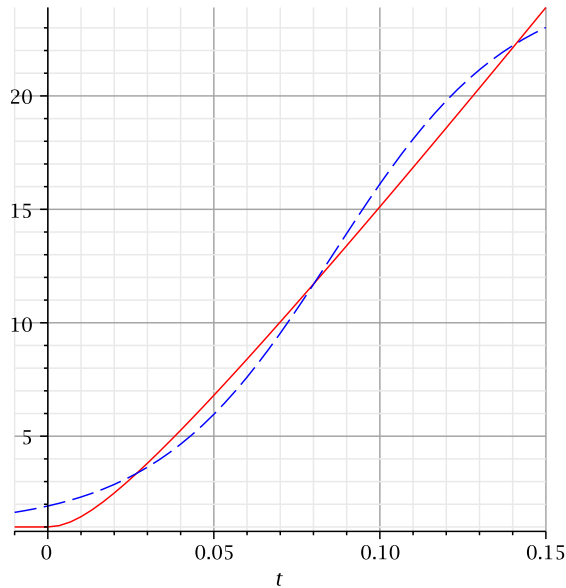
FIG. 14 (color online). The exact scaling function λ (red solid) and its approximation by the tanh function $\tilde{\Omega}_0^2/\Omega$ (blue dashed) over the interval $t = 0.15$ s as described in the text.

$$\omega_\parallel^2(t) = \frac{\omega_\parallel^2(0)}{\lambda^3(t)} - \frac{\ddot{\lambda}(t)}{\lambda(t)}. \qquad (5.34)$$

The necessary trapping frequency is obtained by inserting the desired expansion profile into this expression. One finds that, in fact, the squared trapping frequency becomes negative for a short time near the end of the transition from expansion to staticity indicating a temporarily repulsive force is necessary to stop the BEC from contracting further.

In this way it would be possible to actually create in the lab a BEC system with particular time-dependent trapping frequencies such that the scaling function λ behaves in the way appropriate (as discussed above) to induce the kind of finite expansion or contraction analogue geometry for perturbations. It is worth pointing out again at this point that we expect the general structure of a propagating bump of correlations resulting from a finite scaling to not depend in any crucial way on the fine details of the scaling. We expect the result to be insensitive, for example, to the fact that a precise reproduction of the tanh shape profile is practically very difficult and most probably would only be approximated in any real experiment.

VI. CONCLUSION

In this paper we have considered the correlation structure of expanding BECs both in the idealized case of isotropic and homogeneous expansion as well as in the experimentally relevant case of a finite size, cigar-shaped, BEC anisotropically expanding.

In the first case we have developed a general formalism for probing the effects of particle production on correlations as embodied in the equal-time Wightman function.

Specifically, for any spatially translation invariant system we have shown that it makes sense to define the correlator as in (3.1) which in the case of particle production (using Bogoliubov coefficients) takes the form (4.11). This result is completely generic to particle production in any spatially translation invariant system, applying to standard cosmologies as much as the "analogue spacetimes" of central interest in the current article. Specifically, the general cosmological result was shown to be directly implementable in a $3 + 1$D BEC system with a time-dependent scattering length as well as a $3 + 1$D isotropically expanding BEC, opening two alternative windows on possible observation of this correlation signal.

In the second case (anisotropic BEC) we have shown that the condensate dynamics reduces to an effectively $1 + 1$-dimensional system and that the Wightman function can be generically cast in the form (5.28) for these systems. Using this result we have studied the correlation structure and shown how it carries the signature of analogue cosmological particle production possibly observable in future experiments. In particular, however, we have studied the density correlations in such BEC systems, which are of current experimental interest.

The magnitude of the normalized correlations is of pertinent experimental concern. The overall scale of the propagating bump is given in terms of the normalization factor for phase perturbation along with the additional factors which relate the $1 + 1$D density to the phase field $\frac{\langle \hat{\rho} \, \hat{\rho} \rangle}{\rho^2} \simeq \frac{N}{g^2} \frac{1}{(\rho^{(1+1)})^2} \approx 10^{-7}$. Although this is a very small number, it should be noted that this magnitude is in fact much larger than the magnitude of the background correlation structure (present in flat spacetime also). The relative magnitude of the background to entanglement correlations is independent of the normalization of the mode-function solutions but instead depends on the structure of the Bogoliubov coefficients which derive from the wave equation alone.

The main purpose of this paper was to investigate the characteristic signature related to the cosmological particle emission in an expanding (or more generally time-dependent) BEC, and analyze it without specific attention to its actual measurability. However, one can of course imagine altering the parameters of the background BEC in such a way to improve the signal. For example, one parameter which can be altered by an order of magnitude is the number of atoms N which affects the value of ρ_0 entering into the denominator of the normalized correlations. Another possibility of improving the signal would be to alter the scattering length. We have discussed above the use of the analogue FRW geometry when one induces a time dependence in the scattering length. Here we have something different in mind. Since the background density depends on the scattering length as $a^{3/5}$, by decreasing and holding the scattering length constant before expansion, one might be able to improve the signal. Another

possibility is to choose a longer time scale on which to approximate the eternal expansion with a finite expansion; By stopping the expansion later, the correlations will be propagating on a background density which is lower which would improve the ratio in the normalized correlations. All these ways of altering ρ_0 will also affect the values of η_0, a_i, and a_f possibly giving a more pronounced signal.

A separate analysis should regard the role of a non-vanishing initial temperature of the BEC (or more generally the role of a nonvacuum initial state). In fact, as already pointed out in [9,22,24], the net effect of such an initial temperature (i.e. a ''nonempty'' initial state, but thermally populated) is to significantly increase the quantity of created excitations, therefore enhancing the signal without affecting the mechanism responsible for the particle production. We intend to make further investigations in these directions in future work.

ACKNOWLEDGMENTS

[1] L. Parker, Phys. Rev. **183**, 1057 (1969).
[2] N. D. Birrell and P. C. W. Davies, *Quantum Fields in Curved Space* (Cambridge University Press, Cambridge, UK, 1982).
[3] S. W. Hawking, Nature (London) **248**, 30 (1974).
[4] C. Barcelo, S. Liberati, and M. Visser, Living Rev. Relativity **8**, 12 (2005).
[5] L. J. Garay, J. R. Anglin, J. I. Cirac, and P. Zoller, Phys. Rev. Lett. **85**, 4643 (2000).
[6] C. Barcelo, S. Liberati, and M. Visser, Classical Quantum Gravity **18**, 1137 (2001).
[7] R. Parentani, Phys. Rev. D **82**, 025008 (2010).
[8] R. Balbinot, A. Fabbri, S. Fagnocchi, A. Recati, and I. Carusotto, Phys. Rev. A **78**, 021603 (2008).
[9] I. Carusotto, S. Fagnocchi, A. Recati, R. Balbinot, and A. Fabbri, New J. Phys. **10**, 103001 (2008).
[10] R. Schutzhold and W. G. Unruh, Phys. Rev. D **81**, 124033 (2010).
[11] P. O. Fedichev and U. R. Fischer, Phys. Rev. Lett. **91**, 240407 (2003).
[12] M. Uhlmann, Y. Xu, and R. Schützhold, New J. Phys. **7**, 248 (2005).
[13] U. R. Fischer, Mod. Phys. Lett. A **19**, 1789 (2004).
[14] P. O. Fedichev and U. R. Fischer, Phys. Rev. A **69**, 033602 (2004).
[15] P. O. Fedichev and U. R. Fischer, Phys. Rev. D **69**, 064021 (2004).
[16] R. Schützhold, U. Michael, L. Petersen, H. Schmitz, A. Friedenauer, and T. Schätz, Phys. Rev. Lett. **99**, 201301 (2007).
[17] C. Barcelo, S. Liberati, and M. Visser, Int. J. Mod. Phys. D **12**, 1641 (2003).
[18] C. Barcelo, S. Liberati, and M. Visser, Phys. Rev. A **68**, 053613 (2003).
[19] P. Jain, S. Weinfurtner, M. Visser, and C. W. Gardiner, Phys. Rev. A **76**, 033616 (2007).
[20] M. Visser and S. Weinfurtner, Proc. Sci., QG-PH (2007) 042 [arXiv:0712.0427].
[21] S. Weinfurtner, P. Jain, M. Visser, and C. W. Gardiner, Classical Quantum Gravity **26**, 065012 (2009).
[22] I. Carusotto, R. Balbinot, A. Fabbri, and A. Recati, Eur. Phys. J. D **56**, 391 (2010).
[23] M. Uhlmann, New J. Phys. **12**, 095016 (2010).
[24] S. Manz, R. Bücker, T. Betz, C. Koller, S. Hofferberth, I. E. Mazets, A. Imambekov, E. Demler, A. Perrin, J. Schmiedmayer, and T. Schumm, Phys. Rev. A **81**, 031610 (2010).
[25] A. Imambekov, I. E. Mazets, D. S. Petrov, V. Gritsev, S. Manz, S. Hofferberth, T. Schumm, E. Demler, and J. Schmiedmayer, Phys. Rev. A **80**, 033604 (2009).
[26] D. L. Luxat and A. Griffin, Phys. Rev. A **67**, 043603 (2003).
[27] F. Dalfovo, S. Giorgini, L. P. Pitaevskii, and S. Stringari, Rev. Mod. Phys. **71**, 463 (1999).
[28] M. Visser, arXiv:gr-qc/9311028.
[29] Y. Castin and R. Dum, Phys. Rev. Lett. **77**, 5315 (1996).
[30] V. Gritsev, P. Barmettler, and E. Demler, arXiv:0912.2744.
[31] S. Fulling, *Aspects of Quantum Field Theory in Curved Spacetime* (Cambridge University Press, Cambridge, UK, 1989).
[32] M. Uhlmann, Phys. Rev. A **79**, 033601 (2009).
[33] L. P. Pitaevskii and S. Stringari, *Bose-Einstein Condensation* (Oxford University Press, Oxford, UK, 2003).